

Learning to Compute Ergodic Rate for Multi-cell Scheduling in Massive MIMO

Junchao Shi, *Student Member, IEEE*, Wenjin Wang, *Member, IEEE*, Xinpeng Yi, *Member, IEEE*, Jiaheng Wang, *Senior Member, IEEE*, Xiqi Gao, *Fellow, IEEE*, Qing Liu, and Geoffrey Ye Li, *Fellow, IEEE*

Abstract—In this paper, we investigate multi-cell scheduling for massive multiple-input-multiple-output (MIMO) communications with only statistical channel state information (CSI). The objective of multi-cell scheduling is to activate a subset of users so as to maximize the ergodic sum rate subject to per-cell total transmit power constraint. By adopting beam division multiple access based on the statistical CSI, i.e., channel-coupling matrix (CCM), we simplify multi-cell scheduling as a power control problem in the beam domain, by which the ergodic sum rate is maximized. To reduce the computational burden on finding the ergodic sum rate, we propose a learning-to-compute strategy, which directly computes the complex ergodic rate function from CCMs via a deep neural network. Specifically, by modeling the probability density function of the ordered eigenvalues of the Hermitian CCM matrices as exponential family distributions, a properly designed hybrid neural network makes the ergodic rate computation feasible. With the learning-to-compute strategy, the online computational complexity of multi-cell scheduling is substantially reduced compared with the existing Monte Carlo or deterministic equivalent (DE) based methods while maintaining nearly the same performance.

Index Terms—Beam division multiple access, massive MIMO, neural network, statistical CSI, multi-cell scheduling

I. INTRODUCTION

The massive MIMO powered wireless communication systems have attracted extensive interests in the last decade [2], [3], which improves spectral and energy efficiency by deploying a large number of antennas [4]. The successful applications of massive MIMO [5]–[7] show its promising prospects for future communication networks. With the large-scale antenna arrays at the base station (BS), massive MIMO can serve multiple mobile terminals by reusing time-frequency

This work was supported by the National Key R&D Program of China under Grant 2018YFB1801103, the Jiangsu Province Basic Research Project under Grant SBK2019050020, and the National Natural Science Foundation of China under Grants 61761136016, 61971130 and 61720106003.

This work was presented in part [1] at the International Conference on Wireless Communications and Signal Processing (WCSP), Hangzhou, China, 2018.

J. Shi, W. Wang, J. Wang, and X. Q. Gao are with the National Mobile Communications Research Laboratory, Southeast University, Nanjing 210096, China, and also with the Purple Mountain Laboratories, Nanjing 211100, China (e-mail: jcsht@seu.edu.cn; wangwj@seu.edu.cn; jhwang@seu.edu.cn; xqgao@seu.edu.cn).

X. Yi is with the Department of Electrical Engineering and Electronics, University of Liverpool, L69 3BX, United Kingdom (email: xinpeng.yi@liverpool.ac.uk).

Q. Liu is with the Huawei Technologies Ltd. Company, Shanghai 200120, China (e-mail: patrick.liuqing@huawei.com).

G. Y. Li is with the School of Electrical and Computer Engineering, Georgia Institute of Technology, Atlanta, GA 30332, USA (e-mail: liye@ece.gatech.edu).

physical resource block (PRB), which at the same time also increases the complexity of signal processing.

The availability of CSI at the BS has a significant impact on the throughput of massive MIMO [8], [9]. With channel reciprocity in TDD systems, the downlink channel information is the same as the uplink, which can be estimated through the uplink training. For frequency-division duplex (FDD) systems, instantaneous downlink CSI is usually obtained through downlink training and estimation followed by uplink channel feedback. Meanwhile, the required number of independent pilot symbols for CSI acquisition and the feedback overhead scale with the number of antennas as the BS [10]. As users' mobility increases, channel coherence time becomes relatively short, which imposes more challenges on CSI acquisition. Short coherence time/frequency requires frequent uplink training for TDD and uplink feedback for FDD to adapt to the change of channels. It usually takes a much longer time to acquire accurate CSI in massive MIMO. On the contrary, channel statistics capture the long-term channel characteristics such as spatial correlation. As such, exploiting the statistical CSI for transmission is reasonable, especially in fast fading channels.

Exploiting only statistical CSI for massive MIMO has been investigated recently [11], including beam division multiple access (BDMA) [12] for a single cell. In [12], multiple users with non-overlapping beams are selected for transmission simultaneously. These beams correspond to the eigenmodes of channel transmit covariance matrices, which are asymptotically unique and independent of users' identities, as the number of BS antennas tends to infinity [13], [14]. Multi-cell scheduling aims to activate a subset of users whose beams are not overlapping so that the ergodic sum rate is maximized. However, there are two challenges: (1) Multi-cell scheduling has a combinatorial nature, whose computational complexity scales exponentially with the number of users; (2) No closed-form expressions exist for the computation of ergodic sum rate as a function of CCMs, and thus the performance evaluation of different scheduling strategies incurs prohibitively high complexity. While the existing deterministic equivalent [15] based method achieves the ergodic sum rate approximation with certain accuracy and computational efficiency, the computational complexity and data dependence prohibit it from the real-time user selection scenarios. This motivates us to investigate a learning-to-compute strategy for ergodic rate computation with statistical CSI.

In this paper, we formulate the multi-cell scheduling in massive MIMO as an ergodic rate maximization problem subject to per-cell total transmit power constraint, where the users with

positive power allocation are scheduled for transmission. To make this optimization problem more tractable, we transfer the per-cell power constraint to equal on-off power allocation in the beam domain, i.e., each beam is either allocated with a fixed power (ON) or zero power (OFF), which translates multi-cell scheduling into a beam assignment problem. The performance loss resulted from transferring the original problem into an on-off power allocation one is insignificant as shown in [12]. By this transfer, the follow-up computation of ergodic rate contributes to most of the computational complexity. Thus, we use a neural network to approximate the ergodic rate function from the CCMs to reduce the computational complexity. To summarize, our contributions in this paper are three-fold.

- We develop a learning-to-compute strategy to find the ergodic sum rate by an end-to-end neural network. Different from the approach based on ordered eigenvalues of Wishart matrices in [16], the Hermitian matrix in our work is more complicated than uncorrelated central Wishart matrices. We model the ordered eigenvalues as exponential family distributions, where the rate computation can therefore be addressed by the designed neural networks.
- We formulate a combinatorial optimization problem for multi-cell scheduling, maximizing the weighted ergodic sum rate subject to proper beam assignment that avoids beam overlapping across selected users. Due to the non-linearity of the objective function, we instead develop a greedy approach to solve the integer program efficiently.
- In addition to the maximum sum rate criterion, we take into account the fairness and further propose multi-cell scheduling, compromising efficiency and fairness simultaneously. The corresponding non-convex multi-objective optimization problem maximizes the sum rate and the Jain's index of rate simultaneously.

Simulation results demonstrate the accuracy of the learning-to-compute strategy for ergodic sum rate computation. Our strategy significantly reduces the computational complexity compared with the existing methods but is with near-optimal accuracy. Furthermore, we propose a fairness criterion to ensure fairness with less sum rate loss compared with the existing proportional fairness criterion. Our framework combines the above modules and can schedule users efficiently and fairly.

The rest of this paper is organized as follows. In Section II, we present the system model with beam division multiple access. In Section III, we propose a learning-to-compute strategy for ergodic rate computation, including a hybrid neural network for the general case and a specific neural network for dual-antenna users. In Section IV, we design the scheduling criterion with fairness consideration and propose a K-Best algorithm (KBA) for greedy scheduling. Simulation results are presented in Section V and the paper is concluded in Section VI.

Some of the notations used in this paper are listed as follows:

- Upper and lower case boldface letters denote matrices and column vectors, respectively.

- $\mathbb{C}^{M \times N}$ ($\mathbb{R}^{M \times N}$) denotes the $M \times N$ dimensional complex (real) vector space.
- \mathbf{I}_N denotes the $N \times N$ identity matrix and the subscript is sometimes omitted for brevity.
- $\mathbf{0}$ denotes the all-zero vector (matrix) and $(\cdot)^H$, $(\cdot)^T$, and $(\cdot)^*$ denote conjugate transpose, transpose, and complex conjugate operations, respectively.
- $\mathbb{E}\{\cdot\}$ denotes the expectation operation, $\text{tr}(\cdot)$ and $\det(\cdot)$ represent matrix trace and determinant operations, respectively.
- $\text{bdiag}\{\mathbf{A}_1, \dots, \mathbf{A}_n\}$ denotes a block diagonal matrix with $\mathbf{A}_1, \dots, \mathbf{A}_n$ on the diagonal.
- $[\cdot]_i$ and $[\cdot]_{i,j}$ denote the i -th element of vector and the (i, j) -th element of matrix, respectively.
- $[\mathbf{A}]_i$ denotes the i -th column vector of \mathbf{A} and $[\mathbf{A}]_{\mathcal{B}}$ denotes the sub-matrices of \mathbf{A} consisting of columns specified in \mathcal{B} . $\text{vec}(\mathbf{A})$ denotes the vectorized form of matrix \mathbf{A} .
- $\mathcal{CN}(\boldsymbol{\alpha}, \mathbf{B})$ denotes the circular symmetric complex Gaussian distribution with mean $\boldsymbol{\alpha}$ and covariance \mathbf{B} . \setminus denotes set subtraction operation and $|\mathcal{B}|$ denotes the cardinality of set \mathcal{B} .
- The symbol \odot denotes the Hadamard product of two matrices and the inequality $\mathbf{A} \succeq \mathbf{0}$ means that \mathbf{A} is Hermitian positive semi-definite.

II. MULTI-CELL SCHEDULING FORMULATION

After introducing signal model, we formulate the optimization problem for multi-cell scheduling in this section.

A. Signal Model

Consider downlink transmission of multi-cell multi-user massive MIMO in Fig. 1, consisting of L cells, each with one BS with M transmit antennas. K users are randomly distributed in each cell, where each user is equipped with N receiving antennas. Denote by $\mathbf{x}_{k,\ell} \in \mathbb{C}^{M \times 1}$ the transmitted signal for the k -th user in the ℓ -th cell. The received signal of the k -th user in the j -th cell is given by

$$\mathbf{y}_{k,j} = \sum_{\ell=1}^L \mathbf{H}_{k,j,\ell} \mathbf{x}_{k,\ell} + \mathbf{n}_{k,j} \in \mathbb{C}^{N \times 1}, \quad (1)$$

where $\mathbf{x}_{\ell} = \sum_{k=1}^K \mathbf{x}_{k,\ell}$ is the transmitted signal of the ℓ -th BS, $\mathbf{H}_{k,j,\ell} \in \mathbb{C}^{N \times M}$ denotes the channel from the ℓ -th BS to the k -th user in the j -th cell and $\mathbf{n}_{k,j} \sim \mathcal{CN}(\mathbf{0}, \mathbf{I}_N)$ is the corresponding additive white Gaussian noise vector.

In this paper, we employ the widely-adopted jointly correlated MIMO channel model [17], for which the channel matrix can be decomposed into

$$\mathbf{H}_{k,j,\ell} = \mathbf{U}_{k,j,\ell} \tilde{\mathbf{H}}_{k,j,\ell} \mathbf{V}_{k,j,\ell}^H, \quad (2)$$

where $\tilde{\mathbf{H}}_{k,j,\ell}$ is a random matrix whose entries are independent with zero mean, $\mathbf{U}_{k,j,\ell} \in \mathbb{C}^{N \times N}$ and $\mathbf{V}_{k,j,\ell} \in \mathbb{C}^{M \times M}$ are the eigen matrices on the user side and the base station side, respectively, which are unitary.

With a large scale uniform linear array (ULA) deployed at the BS, $\mathbf{V}_{k,j,\ell}, \forall k, j, \ell$ can be approximated as a unitary

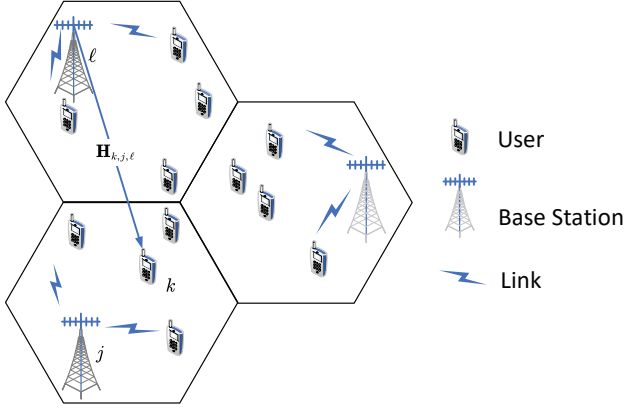


Fig. 1. Downlink transmission of multi-cell multi-user massive MIMO.

discrete Fourier transform (DFT) matrix $\mathbf{F} \in \mathbb{C}^{M \times M}$ [18]. As demonstrated in [19], the correlation matrix, $\mathbf{U}_{k,j,\ell}, \forall k, j, \ell$, in massive MIMO can be regarded as an identity matrix. Thus, we can rewrite the channel matrix in (2) and define the beam domain channel matrix as

$$\tilde{\mathbf{H}}_{k,j,\ell} = \mathbf{H}_{k,j,\ell} \mathbf{F}. \quad (3)$$

It has been shown that BDMA transmission is more preferable for massive MIMO when only statistical CSI is available at the BS [18]. The statistical CSI, i.e. eigenmode channel-coupling matrix in the beam domain [20], is defined as

$$\mathbf{\Omega}_{k,j,\ell} = \mathbb{E} \left\{ \tilde{\mathbf{H}}_{k,j,\ell} \odot \left(\tilde{\mathbf{H}}_{k,j,\ell} \right)^* \right\}, \quad (4)$$

where $\mathbf{\Omega}_{k,j,\ell} \in \mathbb{C}^{N \times M}$. The coefficient, $[\mathbf{\Omega}_{k,j,\ell}]_{nm}$, indicates the average amount of energy that is coupled from the m -th eigenvector of the ℓ -th BS to the n -th eigenvector of the k -th user in the j -th cell. We assume that statistical channel information is available globally at all base stations.

Assumption 1: For multi-cell scheduling, each BS only has access to the channel coupling matrices $\mathbf{\Omega}_{k,j,\ell}, \forall k, j, \ell$.

For beam domain transmission, the received signal can be rewritten as

$$\mathbf{y}_{k,j} = \sum_{\ell=1}^L \tilde{\mathbf{H}}_{k,j,\ell} \mathbf{s}_\ell + \mathbf{n}_{k,j}, \quad (5)$$

where $\mathbf{s}_\ell = \mathbf{F}^H \mathbf{x}_\ell$ ($\mathbf{s}_{k,\ell} = \mathbf{F}^H \mathbf{x}_{k,\ell}$) is the transmitted signal vectors in the beam domain. In (5), the covariance matrix of the transmitted signals, $\mathbb{E} \left\{ \mathbf{s}_{k,\ell} \mathbf{s}_{k,\ell}^H \right\} = \mathbf{\Lambda}_{k,\ell}$, is diagonal, whose entries indicate the transmit powers allocated onto each eigenmode. As in [21], the following ergodic achievable rate for the k -th user in the j -th cell can be derived

$$R_{k,j} = \mathbb{E} \left\{ \log \det \left(\mathbf{I} + \sum_{\ell=1}^L \tilde{\mathbf{H}}_{k,j,\ell} \mathbf{\Lambda}_\ell \tilde{\mathbf{H}}_{k,j,\ell}^H \right) \right\} - \mathbb{E} \left\{ \log \det \left(\mathbf{I} + \sum_{\ell=1}^L \tilde{\mathbf{H}}_{k,j,\ell} \mathbf{\Lambda}_{\ell \setminus (k,j)} \tilde{\mathbf{H}}_{k,j,\ell}^H \right) \right\}, \quad (6)$$

where the expectation takes over the beam domain channel matrix $\tilde{\mathbf{H}}_{k,j,\ell}$, $\mathbf{\Lambda}_\ell = \sum_{k=1}^K \mathbf{\Lambda}_{k,\ell}$ satisfying the per-cell total

power constraint $\text{tr}(\mathbf{\Lambda}_\ell) \leq P_\ell$ and

$$\mathbf{\Lambda}_{\ell \setminus (k,j)} = \begin{cases} \mathbf{\Lambda}_\ell, & \ell \neq j, \\ \mathbf{\Lambda}_\ell - \mathbf{\Lambda}_{k,j}, & \ell = j. \end{cases} \quad (7)$$

B. Problem Formulation

The objective of multi-cell scheduling is to find a set of power allocation matrices $\mathbf{\Lambda}_{1,1}, \dots, \mathbf{\Lambda}_{K,L}$ that maximizes the weighted ergodic sum rate as follows

$$\max_{\mathbf{\Lambda}_{1,1}, \dots, \mathbf{\Lambda}_{K,L}} R_{sum} = \sum_{k,j} \omega_{k,j} R_{k,j}, \quad (8a)$$

$$\text{s.t.} \quad \text{tr}(\mathbf{\Lambda}_\ell) \leq P_\ell, \quad (8b)$$

$$\mathbf{\Lambda}_{k,\ell} \succeq \mathbf{0}, \quad (8c)$$

where $\omega_{k,j} \geq 0$ indicates the priorities of the users for scheduling, and P_ℓ is the total power budget of the ℓ -th cell. It is worth noting that the scheduling parameters are embedded in the power allocation matrices, e.g., the (k,j) -th user is switched off if no power is allocated, i.e., $\mathbf{\Lambda}_{k,j} = \mathbf{0}$.

It has been shown in [18] that the sum rate maximization in the beam domain requires that the activated beams for different users should be non-overlapping, which also applies to the weighted sum rate maximization. Thus, we similarly have the following theorem.

Theorem 1 ([18]): To maximize the weighted ergodic rate in the beam domain, the activated beams for different users should be non-overlapping, i.e., the optimal power allocation in the beam domain of problem (8) satisfies

$$\mathbf{\Lambda}_{k,\ell} \mathbf{\Lambda}_{k',\ell} = \mathbf{0}, \quad \forall k \neq k', \quad (9)$$

where the elements of the diagonal matrix $\mathbf{\Lambda}_{k,\ell}$ indicate the power allocation to the corresponding beams.

Theorem 1 indicates that the beams assigned to both users with non-zero power must be non-overlapping if both users k and k' are scheduled for transmission. For simplicity, we consider equal power allocation across beams. That is, the non-zero elements of power allocation matrix $\mathbf{\Lambda}_\ell$ are equal. Denote indices of the non-zero elements of $\mathbf{\Lambda}_{k,\ell}$ as set $\mathcal{B}_{k,\ell}$, which represents the transmission beam set for the k -th user in the ℓ -th cell. Therefore, we can rewrite the user rate as

$$R_{k,j} = \mathbb{E} \left\{ \log \det \left(\mathbf{I} + \sum_{\ell=1}^L \rho_\ell [\tilde{\mathbf{H}}_{k,j,\ell}]_{\mathcal{B}_\ell} [\tilde{\mathbf{H}}_{k,j,\ell}]_{\mathcal{B}_\ell}^H \right) \right\} - \mathbb{E} \left\{ \log \det \left(\mathbf{I} + \sum_{\ell=1}^L \rho_\ell [\tilde{\mathbf{H}}_{k,j,\ell}]_{\mathcal{B}_{\ell \setminus (k,j)}} [\tilde{\mathbf{H}}_{k,j,\ell}]_{\mathcal{B}_{\ell \setminus (k,j)}}^H \right) \right\}, \quad (10)$$

where $\mathcal{B}_\ell = \bigcup_{k=1}^K \mathcal{B}_{k,\ell}$ is the selected beam set of the ℓ -th cell with

$$\mathcal{B}_{\ell \setminus (k,j)} = \begin{cases} \mathcal{B}_\ell, & \ell \neq j, \\ \mathcal{B}_\ell \setminus \mathcal{B}_{k,j}, & \ell = j, \end{cases} \quad (11)$$

and $\rho_\ell = P_\ell / |\mathcal{B}_\ell|$ is the equal power allocated to each beam in the ℓ -th cell. In addition, considering the fairness of all selected users, we introduce the max number of beams for each user B_{\max} to prevent the users from activating too many beams.

As well-known in the massive MIMO literature [12], users are separable in angle domain if their angle-of-arrivals (AoAs)

are not overlapping. Thus, the maximization problem in (8) can therefore be reformulated in the following way such that no users with overlapping beam sets are scheduled simultaneously, i.e.,

$$\max_{\mathcal{B}_{1,1}, \dots, \mathcal{B}_{K,L}} \sum_{k,j} \omega_{k,j} R_{k,j} \quad (12a)$$

$$\text{s.t. } \mathcal{B}_{k,\ell} \subseteq \mathcal{A}_{k,\ell}, \quad \forall k, \ell \quad (12b)$$

$$\mathcal{B}_{k,\ell} \cap \mathcal{B}_{k',\ell} = \emptyset, \quad k \neq k', \quad (12c)$$

$$|\mathcal{B}_{k,\ell}| \leq B_{\max}, \quad (12d)$$

where $\mathcal{A}_{k,\ell} = \{m \mid \sum_n [\Omega_{k,\ell}]_{nm} \geq \varepsilon_{th}\}$ denotes the set of beams whose energy exceeds a specific threshold ε_{th} , introduced to avoid trivial connection.

There are two challenges on solving this optimization problem. First, multi-cell scheduling is a combinatorial optimization problem [12], [22] and there exists no polynomial-time complexity algorithm to solve it accurately [23]. Second, accurately computing ergodic rate is intractable because of the unknown joint distribution of channel statistics. Since the ergodic sum rate should be computed repeatedly, it contributes to the majority of complexity for existing numerical methods, such as the deterministic equivalent [15] based method. To address the challenge, we develop a learn-to-compute strategy in Section III to find ergodic rate for scheduling.

III. LEARNING-TO-COMPUTE STRATEGY FOR ERGODIC RATE COMPUTATION

In this section, we develop the efficient learning-to-compute strategy for ergodic rate computation based on neural networks, including a hybrid neural network for general case and a specific neural network for dual-antenna users.

A. General Strategy: Hybrid Neural Network

We focus on the general case for ergodic rate computation and learn a function to approximate (6), which includes (10) as a special case. Let $\Lambda_s = \text{bdiag}\{\Lambda_1, \dots, \Lambda_L\} \in \mathbb{C}^{ML \times ML}$, $\Lambda_{s \setminus (k,j)} = \text{bdiag}\{\Lambda_1 \setminus (k,j), \dots, \Lambda_L \setminus (k,j)\} \in \mathbb{C}^{ML \times ML}$, $\tilde{\mathbf{H}}_{k,j} = [\tilde{\mathbf{H}}_{k,j,1} \ \mathbf{H}_{k,j,2} \ \dots \ \tilde{\mathbf{H}}_{k,j,L}] \in \mathbb{C}^{N \times ML}$, $\Omega_{k,j} = [\Omega_{k,j,1} \ \Omega_{k,j,2} \ \dots \ \Omega_{k,j,L}] \in \mathbb{C}^{N \times ML}$, and the rate of the k -th user in the j -th cell in (6) can also be written as

$$R_{k,j} = \mathbb{E} \left\{ \log \det \left(\mathbf{I} + \tilde{\mathbf{H}}_{k,j} \Lambda_s \tilde{\mathbf{H}}_{k,j}^H \right) \right\} - \mathbb{E} \left\{ \log \det \left(\mathbf{I} + \tilde{\mathbf{H}}_{k,j} \Lambda_{s \setminus (k,j)} \tilde{\mathbf{H}}_{k,j}^H \right) \right\}. \quad (13)$$

The objective is to approximate the common ergodic rate

$$\mathcal{I}_{k,j}(\Lambda) = \mathbb{E} \left\{ \log \det \left(\mathbf{I} + \tilde{\mathbf{H}}_{k,j} \Lambda \tilde{\mathbf{H}}_{k,j}^H \right) \right\}, \quad (14)$$

given the power allocation matrix Λ and the corresponding CSI $\Omega_{k,j}$. Due to the element-wise correspondence between the elements of $\tilde{\mathbf{H}}_{k,j}$ and $\Omega_{k,j}$, the objective $\mathcal{I}_{k,j}(\Lambda)$ is only relevant to the matrix obtained by multiplying CCM by the corresponding power, i.e., the matrix $\Omega_{k,j} \Lambda$. We omit k and j in the subscript hereafter for brevity.

In this paper, we focus on the Rayleigh fading. However, the results can be easily extended to other channel models.

For example, for the Rician fading, the only difference in ergodic rate computation is that the input of the neural network involves additional channel mean information while the structure of neural networks remains unchanged. To simplify neural network design, we introduce the matrix $\mathbf{X} \in \mathbb{C}^{N \times ML}$ as

$$\mathbf{X} = f_{\mathbf{X}}(\Omega, \Lambda) = \Omega \Lambda. \quad (15)$$

A common approach on function approximation using deep neural networks (e.g., feed-forward neural network (FNN) and convolutional neural network (CNN) [24]) is to learn the weight parameters by training the network with sample input \mathbf{X} and the corresponding labels/output \mathcal{I} . The feasibility of such an approach has been demonstrated by the universal approximation theorem [25], [26], for which a single hidden layer feed-forward network with a sufficiently large number of neurons can approach arbitrary continuous function well on the compact subset of \mathbb{R}^n . Similarly, the convolutional neural network can approximate arbitrary continuous function with arbitrary accuracy as long as the depth of the neural network is large enough [27]. Both of the above neural networks are pure data-driven, where the approximation performance highly depends on the training data, i.e., channel matrix samples.

On the contrary, the ergodic rate function is continuous over the probability space of channel statistics, such that the finite sampled channel matrices are not able to characterize it accurately. Thus, it is not surprising that the generalization performance using sampled channel matrices as the training data set is unsatisfactory. In addition, simply using channel matrices as input and rate as output totally ignores channel characteristics, which is the dominant factor of the ergodic rate function. Thus, pure data-driven networks usually require deeper and wider architectures for the purpose of over parameterization.

In order to alleviate the limitation, we propose a model-driven neural network architecture, which consists of two major components: 1) instead of using instantaneous channel matrices samples, we apply channel statistics (i.e., $\Omega_{k,j}$) as the input; 2) we extract internal features with implicit probability distribution information from channel statistics, followed by ergodic rate computation through these internal features. In doing so, we do not need to generate a large size of channel matrices for training, and the internal feature extraction lends itself to a simpler network architecture with higher accuracy. Before the network design, in what follows we first describe how we extract the internal features. The ergodic rate in (14) can be rewritten as

$$\mathcal{I}(\Lambda) = \sum_{n=1}^N \int \log(1 + \lambda_n) p(\lambda_n) d\lambda_n, \quad (16)$$

where λ_n denotes the n -th eigenvalues of $\tilde{\mathbf{H}} \Lambda \tilde{\mathbf{H}}^H$ and $p(\lambda_n)$ is the probability density function of λ_n . These eigenvalues are arranged in the descending order. The distribution of eigenvalues, λ_n 's, encompass all information of CSI to compute the ergodic rate. However, due to the complexity of the probability distribution of the matrix $\tilde{\mathbf{H}} \Lambda \tilde{\mathbf{H}}^H$, there is no analytical method available in the literature to estimate $p(\lambda_n)$ directly. According to the well-known Pitman-

Koopman-Darmois Theorem [28], exponential is the only family of probability distributions with domain independent of the estimated parameter with a sufficient statistic that is dimension-bounded as sample size increases. As the input \mathbf{X} is finite in dimension, we model λ_n as an exponential family distribution, which can be written in the form

$$p(\lambda_n) = q(\lambda_n) g(\boldsymbol{\eta}) \exp\{\boldsymbol{\eta}^T \mathbf{t}(\lambda_n)\}, \quad (17)$$

where $q(\lambda_n)$ is called the underlying measure, $\boldsymbol{\eta}$ is called the natural parameter, $g(\boldsymbol{\eta}) = 1/\int q(\lambda_n) \exp\{\boldsymbol{\eta}^T \mathbf{t}(\lambda_n)\} d\lambda_n$ is a normalization factor, and $\mathbf{t}(x)$ is the sufficient statistic of the distribution. Thus, the origin moment vector

$$\mathbf{m}_i = \mathbb{E}\{\mathbf{t}(\lambda_n)\} \quad (18)$$

encompasses all of the information regarding the data related to the parameter $\boldsymbol{\eta}$. According to Taylor series, we introduce the first P -order origin moment to approximate $\mathbf{t}(\lambda_n)$, i.e.,

$$\mathbf{t}(\lambda_n) \approx [\lambda_n \lambda_n^2 \dots \lambda_n^P]^T, \quad (19)$$

where P is an adjustable parameter. Denote $\mathbf{m} = [\mathbf{m}_1^T \mathbf{m}_2^T \dots \mathbf{m}_N^T]^T \in \mathbb{C}^{NP \times 1}$ and $\mathbf{c} = [c_1 c_2 \dots c_N]^T \in \mathbb{C}^{N \times 1}$, where c_n represents the ergodic rate component corresponding to the n -th ordered eigenvalue

$$c_n = \int \log(1 + \lambda_n) p(\lambda_n) d\lambda_n. \quad (20)$$

Since the two-dimensional input matrix \mathbf{X} is sparse as the beam is energy-concentrated and the power differs in beams due to different channel conditions, we adopt a CNN for feature extraction. The convolutional neural networks process data with a grid-like structure [24] and have been tremendously successful in practical applications [29]. The CNN consists of several convolution modules, a flatten layer and several fully-connected layers. Each convolution module is composed of a convolution layer, a activation layer that removes negative values to increase non-linearity, e.g. rectified linear unit (ReLU) [30], and a pooling layer for non-linear down-sampling, e.g., max pooling [31]. Finally, the fully-connected layers accomplish advanced reasoning. The objective function is also relevant to SNR, so it functions as an input of the neural network at the fully-connected layer. In addition, as the statistics vector, \mathbf{m} , is generally not sparse and its dimension is relatively low, we utilize FNN to realize the part of ergodic rate computation. As such, we construct a hybrid neural network (HNN), as shown in Fig. 2, by appending an FNN to a CNN to approximate the ergodic rate function.

Thus, the computation of ergodic rate can be decomposed into two steps:

- 1) *Encoder*: A CNN to encode the input matrix \mathbf{X} as hidden layer feature \mathbf{m} , i.e., the statistics of eigenvalues.
- 2) *Decoder*: An FNN to decode the hidden layer feature \mathbf{m} as rate vector \mathbf{c} , whose elements can then be added up to get the ergodic rate \mathcal{I} .

By decomposing the objective function into two relatively simple ones and reducing the complexity of the learning model, the number of neurons and training data required can be reduced. Compared with two pure data-driven neural

networks, the proposed network not only improves generalization performance but also considerably reduces computational complexity. Noting that the hybrid neural network can be adapted to various antennas, cells, and users configurations.

Denote by $\mathcal{I}_h(\mathbf{w}_h, \mathbf{X})$ the sum of the HNN output, where the set of all weight and bias parameters have been grouped together into a vector \mathbf{w}_h . Once parameters vector, \mathbf{w}_h , is trained, we can obtain the approximated function of ergodic rate. To this end, we first generate two training sets $\mathcal{E} = \{(\mathbf{X}^{(i)}, \mathbf{m}^{(i)}) \mid i = 1, \dots, N_{\mathcal{E}}\}$ and $\mathcal{D} = \{(\mathbf{m}^{(i)}, \mathbf{c}^{(i)}) \mid i = 1, \dots, N_{\mathcal{D}}\}$ by the Monte-Carlo method (see section V-A). Second, the neural networks will be trained based on \mathcal{E} and \mathcal{D} , respectively, to obtain the optimal weights vector, \mathbf{w}_h^{\diamond} . The loss functions are given by

$$\mathcal{L}_{\mathcal{E}} = \frac{1}{N_{\mathcal{E}}} \sum_{i=1}^{N_{\mathcal{E}}} \|\mathbf{m}^{(i)} - \hat{\mathbf{m}}^{(i)}\|^2, \quad \mathcal{L}_{\mathcal{D}} = \frac{1}{N_{\mathcal{D}}} \sum_{i=1}^{N_{\mathcal{D}}} \|\mathbf{c}^{(i)} - \hat{\mathbf{c}}^{(i)}\|^2, \quad (21)$$

where $\hat{\mathbf{m}}^{(i)}$ and $\hat{\mathbf{c}}^{(i)}$ are the predicted results of the encoder and the decoder. In order to improve generalization performance, a large training set is required but simultaneously results in expensive computational cost. Thus, we employ the widely-used stochastic gradient descent (SGD) [24], which extracts a minibatch of samples uniformly from the training set during each iteration. Further, the procedures of dropout [32] are used to avoid over-fitting.

Finally, with the reshaped input data as

$$\mathbf{X}_{s,k,j} = f_{\mathbf{X}}(\boldsymbol{\Omega}_{k,j}, \boldsymbol{\Lambda}_s), \quad \mathbf{X}_{s \setminus (k,j)} = f_{\mathbf{X}}(\boldsymbol{\Omega}_{k,j}, \boldsymbol{\Lambda}_{s \setminus (k,j)}), \quad (22)$$

the ergodic rate of the k -th user in the j -th cell can be computed immediately by

$$R_{k,j}^{hnn} = \mathcal{I}_h(\mathbf{w}_h^{\diamond}, \mathbf{X}_{s,k,j}) - \mathcal{I}_h(\mathbf{w}_h^{\diamond}, \mathbf{X}_{s \setminus (k,j)}). \quad (23)$$

B. Specific Neural Network for Dual-Antenna Users

Dual-antenna user terminals are perhaps more popular than any other case. For dual-antenna users, i.e., $N = 2$, we propose a refined input by mining in-depth statistical characteristics to further reduce the computational complexity. The refined inputs are due to the following theorem, proved in Appendix A.

Theorem 2: When $N = 2$, the first-order statistic of matrix $\tilde{\mathbf{H}}\boldsymbol{\Lambda}\tilde{\mathbf{H}}^H$ satisfies the following equations.

$$\mathbb{E}(\lambda_1 + \lambda_2) = \sum_n \sum_m [\mathbf{X}]_{nm}, \quad (24)$$

$$\mathbb{E}(\lambda_1 \lambda_2) = \prod_n \sum_m [\mathbf{X}]_{nm} - \sum_m \prod_n [\mathbf{X}]_{nm}. \quad (25)$$

Remark 1: Theorem 2 establishes the relation between the refined input (i.e., first-order statistic of matrix $\tilde{\mathbf{H}}\boldsymbol{\Lambda}\tilde{\mathbf{H}}^H$) and the original one (i.e, statistical CSI and power allocation). As such, we define the refined input as

$$\mathbf{s} = f_s(\boldsymbol{\Omega}, \boldsymbol{\Lambda}) = [\mathbb{E}(\lambda_1 + \lambda_2) \quad \mathbb{E}(\lambda_1 \lambda_2)]^T \in \mathbb{C}^{2 \times 1}. \quad (26)$$

By choosing the origin moment order $P = 1$, which is accurate enough to approximate $p(\lambda_n)$ from the simulation in III-A, the learning objective turns

$$\mathbf{m} = [\mathbb{E}(\lambda_1) \quad \mathbb{E}(\lambda_2)]^T \in \mathbb{C}^{2 \times 1}. \quad (27)$$

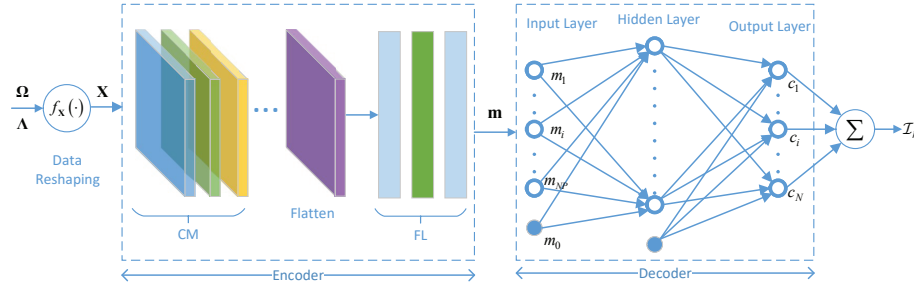


Fig. 2. The proposed hybrid neural network for ergodic rate computation.

One feasible method is to compute the objective, \mathbf{m} , from the vector, \mathbf{s} . The refined input has several attractive benefits. The most important one is that its dimension is independent of the number of the BS antennas, M and the number of cells, L . Thanks to this characteristic, the neural network will remain on a small scale, which reduces not only the complexity of offline training and saves storage costs, but also that of online computing. When $N = 2$, HNN reduces to a fully connected NN, i.e., the specific neural network (SNN) shown in Fig. 3. Both of the encoder and decoder are realized by FNN because of the low dimension of input \mathbf{s} and statistics vector \mathbf{m} . Notice that the number of units in the hidden layers can usually be relatively small. Noting that the SNN is specifically designed for dual-antenna users. In other cases, we can still utilize HNN to achieve the near-optimal sum rate while maintaining the relatively low computational complexity.

Denote by $\mathcal{I}_s(\mathbf{w}_s, \mathbf{s})$ the sum of the output of SNN given the weights vector \mathbf{w}_s and the input vector \mathbf{s} . First, generate two training sets $\mathcal{S} = \{(\mathbf{s}^{(i)}, \mathbf{m}^{(i)}) | i = 1, \dots, N_S\}$ and $\mathcal{D} = \{(\mathbf{m}^{(i)}, \mathbf{c}^{(i)}) | i = 1, \dots, N_D\}$ utilizing the Monte-Carlo method. Second, train the neural networks based on \mathcal{S} and \mathcal{D} respectively to obtain the optimal weights vector \mathbf{w}_s^\diamond and thus obtain the approximated ergodic rate function, $\mathcal{I}(\mathbf{w}_s^\diamond, \mathbf{s})$. Finally, with the reshaped input data as

$$\mathbf{s}_{s,k,j} = \mathbf{s}(\boldsymbol{\Omega}_{k,j}, \mathbf{\Lambda}_s), \mathbf{s}_{s \setminus (k,j)} = \mathbf{s}(\boldsymbol{\Omega}_{k,j}, \mathbf{\Lambda}_{s \setminus (k,j)}), \quad (28)$$

the rate of k -th user in the j -th cell can be computed immediately by

$$R_{k,j}^{snn} = \mathcal{I}_s(\mathbf{w}_s^\diamond, \mathbf{s}_{s,k,j}) - \mathcal{I}_s(\mathbf{w}_s^\diamond, \mathbf{s}_{s \setminus (k,j)}). \quad (29)$$

IV. EFFICIENT AND FAIR SCHEDULING

With ergodic rate computation in Section III, we can address the scheduling problem discussed in Section II. To strike a balance between overall system performance and user fairness, a common approach is to adopt proportional fairness criterion [33], [34] with the weights $\omega_{k,j}$ as aiming at the sum rate maximization incurs some unfairness issues, e.g., the users with poor channel quality may not be served in an enough period. Recent works have proposed several approaches to balance efficiency and fairness [35], [36]. In [37], five axioms for fairness measures in resource allocation are presented together with a family of fairness measures satisfying the axioms, providing an analytical way of choosing the fairness measures. Beyond weighted sum rate maximization, we formulate the

multi-cell scheduling taking both max-min and Jain's fairness into consideration in this section.

A. Weighted Sum Rate Maximization

In order to translate the qualitative formulation in (12) into a quantitative one, we introduce a set of binary variables $\{z_{m,k,\ell}\}$ to indicate if the m -th beam of the ℓ -th BS is active for the k -th user, i.e.,

$$z_{m,k,\ell} = \begin{cases} 1, & \text{if } [\mathbf{\Lambda}_{k,\ell}]_{m,m} > 0, \\ 0, & \text{otherwise.} \end{cases} \quad (30)$$

Further, we introduce a binary matrix $\mathbf{A}_\ell \in \{0,1\}^{M \times K}$ to capture the strong user-beam links for which the effective channel quality of users on such beams exceeds a predetermined threshold. As such, the optimization problem in (12) can be reformulated into a quantitative nonlinear integer program.

$$\max_{\{z_{m,k,\ell}\}} \sum_{k,j} \omega_{k,j} R_{k,j}, \quad (31a)$$

$$\text{s.t. } z_{m,k,\ell} \leq [\mathbf{A}_\ell]_{m,k}, \quad \forall m, k, \ell, \quad (31b)$$

$$\sum_k z_{m,k,\ell} \leq 1, \quad \forall m, \ell, \quad (31c)$$

$$\sum_m z_{m,k,\ell} \leq B_{max}, \quad \forall k, \ell, \quad (31d)$$

$$z_{m,k,\ell} \in \{0,1\}, \quad \forall m, k, \ell, \quad (31e)$$

where (31b) guarantees that only user-beam links with high quality can be the candidates for assignment, (31c) ensures that each beam can only be assigned to at most one user for which the users with no beam assigned will be switched off, (31d) ensures that each user can only occupy at most B_{max} beams to prohibit a user from occupying too many resources, and the ergodic rate $R_{k,j}$ can be rewritten as

$$R_{k,j} = \mathbb{E} \left\{ \log \det \left(\mathbf{I} + \sum_{m,k,\ell} \rho_\ell \boldsymbol{\Xi}_{m,k,j,\ell} z_{m,k,\ell} \right) \right\} \\ - \mathbb{E} \left\{ \log \det \left(\mathbf{I} + \sum_m \sum_{(k',\ell') \neq (k,j)} \rho_{\ell'} \boldsymbol{\Xi}_{m,k',j,\ell'} z_{m,k',\ell'} \right) \right\}, \quad (32)$$

where $\rho_\ell = P_\ell / \sum_{m,k} z_{m,k,\ell}$, $\boldsymbol{\Xi}_{m,k,j,\ell} = \tilde{\mathbf{h}}_{m,k,j,\ell} \tilde{\mathbf{h}}_{m,k,j,\ell}^H$ and $\tilde{\mathbf{h}}_{m,k,j,\ell}$ is the m -th column of $\mathbf{H}_{k,j,\ell}$.

It is not hard to verify that (31) is equivalent to (12). Thanks to the ergodic rate maximization, multi-cell scheduling is implicitly done through beam assignment, where the users with

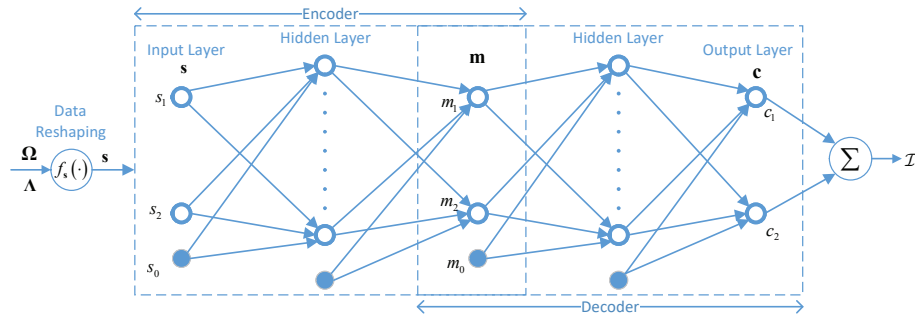


Fig. 3. The proposed specific neural network diagram for ergodic rate computation with $N = 2$.

less contribution to ergodic rate will not be assigned any beams and therefore not be scheduled. It turns out such an implicit multi-cell scheduling is effective because the beam-centric assignment strategy pushes user selection towards ergodic rate maximization.

Algorithm 1 KBA for multi-cell scheduling

Input: The eigenmode channel-coupling matrix $\Omega_{k,j,\ell}, \forall k, j, \ell$.
Output: The user set \mathcal{U} and beam indices $z_{m,k,\ell}$.
1: Initialize user set $\mathcal{U} = \emptyset$ and beam indices $z_{m,k,\ell} = 0, \forall m, k, \ell$.
2: **for** $|\mathcal{U}| \leq KL$ **do**
3: **for** $u \notin \mathcal{U}$ **do**
4: **for** $b \leq B_{max}$ **do**
5: Assign b energy-strongest inactive beams to u .
6: Compute the ergodic rates $R_{k,j}(\mathcal{U} \cup \{u\}), \forall k, j$ by the properly trained hybrid neural network.
7: Compute the objective f_o and constraint f_c for evaluation
8: **if** f_o decreases **then**
9: break
10: **end if**
11: **end for**
12: **end for**
13: **if** problem (33) has solution **then**
14: Update $\mathcal{U} \leftarrow \mathcal{U} \cup \{u\}$
15: Set $z_{m,k,\ell} = 1$ according to the beam assignment
16: **else**
17: Goto 20
18: **end if**
19: **end for**
20: Return \mathcal{U} and $\{z_{m,k,\ell}\}$.

A closer inspection reveals that the constraints in reformulation (31) are those of bipartite b -matching problems (also known as semi-assignment problems) [38], a special case of the transportation problem for which there exists strongly polynomial algorithms [39]. However, the objective function in (31) is nonlinear and involves a neural network for ergodic rate computation, and therefore it is extremely challenging to solve it accurately. Instead, we employ the low-complexity K-Best algorithm (KBA) as shown in Algorithm 1, which adds users in a greedy fashion until the sum rate no longer increases, i.e.,

$$\begin{aligned} \max_{u \notin \mathcal{U}} f_o &= R_{sum}(\mathcal{U} \cup \{u\}), \\ \text{s.t. } f_c &= R_{sum}(\mathcal{U}) - R_{sum}(\mathcal{U} \cup \{u\}) \leq 0. \end{aligned} \quad (33)$$

where f_o and f_c denote the objective and the constraint function in each iteration, $R_{sum}(\mathcal{U})$ denotes the sum rate of the users in set \mathcal{U} . The k -th user in the j -th cell is active if $\sum_m z_{m,k,j} > 0$ and the m -th beam of the ℓ -th cell is active if

$\sum_k z_{m,k,\ell} > 0$. During the iterations, each user selects several beams with the strongest energy. The index of the energy-strongest beam of the j -BS for the k -th user in the j -th cell is defined as

$$m_{k,j,j}^\diamond = \arg \max_m \sum_n [\Omega_{k,j,j}]_{nm}. \quad (34)$$

B. Max-Min Fairness

In order to ensure the fairness, we maximize the achievable rate of the worst-case user [40]. Thus, the optimization problem can be formulated as

$$\begin{aligned} \max_{\Lambda_{1,1}, \dots, \Lambda_{K,L}} \min_{k,j} (\omega_{k,j} R_{k,j}), \\ \text{s.t. } \text{tr}(\Lambda_\ell) \leq P_\ell, \\ \Lambda_{k,\ell} \succeq \mathbf{0}. \end{aligned} \quad (35)$$

To analyze the optimal solution to the above problem, the following lemma, proved in Appendix B, is essential.

Lemma 1: Let \mathbf{A} , \mathbf{B} , and \mathbf{C} be positive definite $N \times N$ matrices.

i) The function

$$f(x) = \log \det(\mathbf{B} + x\mathbf{A}) \quad (36)$$

increases monotonously with x on $x \geq 0$;

ii) The function

$$g(x) = \log \det(\mathbf{B} + x\mathbf{A}) - \log \det(\mathbf{C} + x\mathbf{A}) \quad (37)$$

decreases monotonously with x on $x \geq 0$, if $\mathbf{B} \succ \mathbf{C}$.

Based on Lemma 1, we can obtain the following lemma for analyzing the optimal solution to problem (35) in Appendix C.

Lemma 2: All users have the same weighted rate by max-min fairness, i.e., the optimal rates $\{R_{k,j}^\diamond\}$ in (35) satisfy

$$\omega_{k,j} R_{k,j}^\diamond = \omega_{i,\ell} R_{i,\ell}^\diamond, \forall k, j, i, \ell. \quad (38)$$

Lemma 2 shows that if all users have the same priority, max-min fairness prefers to schedule all users. The characteristic of equal rate can be utilized in the measurement of fairness subsequently.

C. Jain's Fairness

While max-min fairness is prone to the balance between the individual rate and the priorities/weights, it may not lead to

maximal sum rate because of the lack of multi-cell scheduling. Therefore, we introduce Jain's fairness, which satisfies a series of axioms consisting of continuity and homogeneity, etc. [37].

Definition 1 (Jain's Index [41]): Jain's index of rate is given by

$$J_R = \left(\sum_{k,j} R_{k,j} \right)^2 / \left(KL \sum_{k,j} R_{k,j}^2 \right). \quad (39)$$

The Jain's index of rate measures fairness by indicating the proportion of the users who are scheduled with the equal rate. Note that maximizing Jain's index alone will lead to max-min fairness. Thus, to avoid that, we maximize the sum rate at the same time subject to multi-cell scheduling, i.e., maximize the objectives (R_{sum}, J_R) . Multi-objective optimization targets Pareto optimal solutions/points, for which increasing one objective will inevitably decrease another one. We have Pareto points [42] defined as follows.

Definition 2 (Pareto Points): User set \mathcal{U}_s^\diamond and beam sets $\mathcal{B}_i^\diamond, i \in \mathcal{U}_s^\diamond$ is a Pareto point if there are no other \mathcal{U}_s and $\mathcal{B}_i, i \in \mathcal{U}_s$, such that the corresponding sum rate and Jain's index simultaneously satisfy $R_{sum} \geq R_{sum}^\diamond$ and $J_R \geq J_R^\diamond$, where the equalities do not hold simultaneously.

Definition 2 indicates that none of the objective functions can be improved in value without degrading some of the other objective values. There are several methods on finding the Pareto points of a multi-objective problem, e.g., weighted sum method, Epsilon-constraint method and Hybrid method [43]. Employing the Epsilon-constraint method, we reformulate the maximization problem as

$$\begin{aligned} \max_{\{z_{m,k,\ell}\} \subseteq \mathcal{Z}} \quad & J_R, \\ \text{s.t.} \quad & R_{sum} \geq R_{th}. \end{aligned} \quad (40)$$

where set \mathcal{Z} denotes the domain satisfying (31b)-(31e), R_{th} is the minimal sum rate demanded for these cells of interest. Given the minimum sum rate guarantee, we aim to ensure fairness for the communication system. In addition, various sum rate requirements can be adapted by dynamically adjusting constraint R_{th} . Notice that all Pareto points can be found by changing the constraint R_{th} .

Problem (40) can also be solved by applying Algorithm 1. We first search user and beam set to maximize the sum rate and then add users in a greedy fashion before the sum rate drops below the threshold. In this step, we can obtain the maximum sum rate, R_{max} , as a reference value for threshold setting. In the update process, we maximize Jain' index under the sum rate constraint, i.e., change the update condition in (33) as

$$\begin{aligned} \max_{u \notin \mathcal{U}} \quad & f_o = J_R(\mathcal{U} \cup \{u\}), \\ \text{s.t.} \quad & f_c = R_{th} - R_{sum}(\mathcal{U} \cup \{u\}) \leq 0. \end{aligned} \quad (41)$$

The larger R_{th} is, the more inclined the algorithm is to maximize the sum rate while the smaller R_{th} motivates the algorithm concern more with the fairness. When R_{th} exceeds the maximum sum rate R_{max} , the KBA degenerates to sum rate maximization.

V. SIMULATION RESULTS

In this section, we present the simulation results to evaluate the performance of the proposed algorithms using the WINNER II channel model [44], which has been validated by measured data and commonly used to train neural networks in wireless communication applications [22]. In particular, we consider a wide band system consisting of $L = 3$ cells, each with one base station (BS) with $M = 128$ antennas. $K = 40$ users are randomly distributed in each cell, where each user is equipped with $N = 2$ antennas. The CCMs are obtained through 12 samples and 1200 sub-carriers, which is enough for accuracy shown in [12]. For the WINNER II model, we consider the C1 (Suburban) simulation scenario in [44] and utilize the DFT matrix to transform channels into beam domain.

A. Data Set Generation: Monte-Carlo Method

We generate channel samples by widely-used WINNER II, which is enough to capture the feature of the practical wireless channels. The labels are computed by Monte-Carlo methods, which solves deterministic problems with randomness. The set of training and test samples are different subsets of the generated CCM set. The computational process can be summarized into three main steps:

1) *Modeling:* According to the first and second orders of channel statistics, we model the channel by a constant multiplied by a standard Gaussian random variable. Then the matrix form of the random channel from the ℓ -th BS to the k -th user in the j -th cell can be written as

$$\mathbf{G}_{k,j,\ell} = \mathbf{M}_{k,j,\ell} \odot \mathbf{W}_{k,j,\ell}, \quad (42)$$

where $\mathbf{W}_{k,j,\ell}$ is a complex Gaussian random matrix of independent identical distribution (i.i.d.) entries with zero mean and unit variance, and $\mathbf{M}_{k,j,\ell}$ is an $N \times M$ deterministic matrix with nonnegative elements satisfying $\Omega_{k,j,\ell} = \mathbf{M}_{k,j,\ell} \odot \mathbf{M}_{k,j,\ell}^*$.

2) *Generating Realizations:* Given the above modeling, we generate channel realizations $\mathcal{G} = \{\mathbf{G}_{k,j,\ell}^{(i)} | i = 1, \dots, N_G\}$.

3) *Labeling:* For brevity, we omit k and j in the subscript hereafter. From the generated dataset, we can compute the empirical average to approximate the stochastic mean, i.e.,

$$\mathbf{m}_n = \frac{1}{N_G} \sum_{i=1}^{N_G} \mathbf{t}(\hat{\lambda}_n^{(i)}), \quad (43)$$

$$c_n = \frac{1}{N_G} \sum_{i=1}^{N_G} \log(1 + \hat{\lambda}_n^{(i)}), \quad (44)$$

$$\mathcal{I}(\Lambda) = \frac{1}{N_G} \sum_{i=1}^{N_G} \left\{ \log \det \left(\mathbf{I} + \mathbf{G}^{(i)} \Lambda (\mathbf{G}^{(i)})^H \right) \right\}, \quad (45)$$

where $\hat{\lambda}_n^{(i)}$ denotes the n -th eigenvalues of $\mathbf{G}^{(i)} \Lambda (\mathbf{G}^{(i)})^H$. With a sufficiently large number of samples, the empirical mean approximates the expectation well. By utilizing (15), (43)-(45), we can generate the data sets of proposed neural networks. Fig. 4 illustrates the graphical workflow of dataset generation. The training is conducted off-line and it is unnecessary to be re-trained by the original large data set when the channel statistics vary. To fairly compare the performance,

training datasets for different neural networks are generated with the same channel samples.

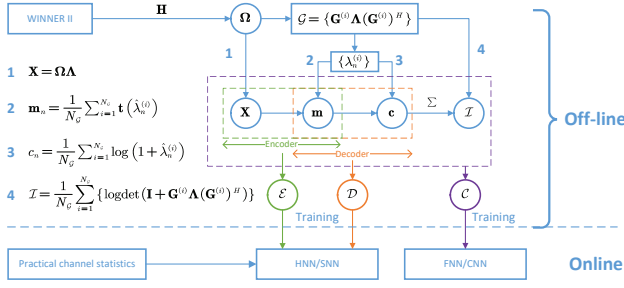


Fig. 4. The graphical workflow of dataset generation.

To enhance the generalization performance, we generate the data set by taking into account various channel scenarios, such as different SNRs, user distributions, mobile speeds, and etc. It is worth mentioning that the channel samples are not limited to be generated by WINNER II but also can be practically measured online [45] to improve the generalization performance (e.g. transfer learning [46]). Thus, the trained neural network can adapt to various practical scenarios. As the training is conducted off-line, enough samples can be generated for training and a sufficiently large N_G in each sample generation can be set to approach the near-optimal expectation. In this paper, we set the size of the training data sets $N_E = N_D = 640,000$ and the number of random channels in each sample $N_G = 100$.

B. Evaluation of Rate Computation

Given the training sets generated by the Monte-Carlo method, we take Monte-Carlo simulation (MS) in (45) as the benchmark to evaluate the sum rate computed by the neural network. The existing deterministic equivalent (DE) method is also presented here as a baseline. With the same dropout (0.5), other major parameters of FNN and CNN are shown in Table I. With regard to HNN (or SNN), as the parameters of encoder and decoder are constructed by CNN and FNN, the above parameters are reused. Fig. 5 compares sum rates versus signal-to-noise ratios (SNR). The HNN and SNN approach near-optimal performance while the traditional FNN and CNN are unsatisfactory. As the data reshaping process may lead to the loss of information, HNN is slightly better than SNN. However, data reshaping also brings about the sharp reduction of computational complexity, which will be discussed later in detail, together with the relationship between FNN and CNN.

TABLE I
MAJOR PARAMETERS OF NEURAL NETWORKS

Model	Learning Rate	Batch Size	Training Steps
FNN	0.001	512	16,000
CNN	0.000,1	1,024	10,000

Table II illustrates the complexity of rate computation algorithms. Notice that N_k , S_k , and S_p denote number of

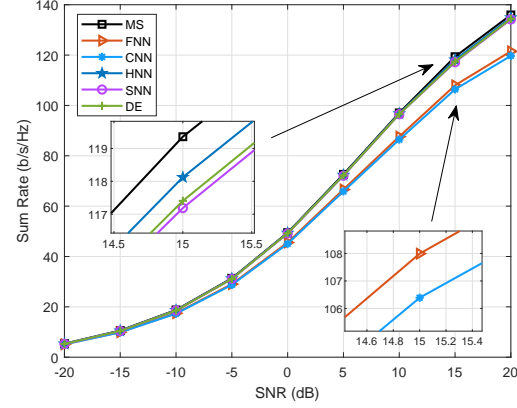


Fig. 5. Sum rate versus SNR with respect to different rate computation algorithms.

TABLE II
COMPARISON OF COMPLEXITY BETWEEN DIFFERENT RATE COMPUTATION ALGORITHM

Algorithm	Complexity	Typical Value
MC	$O(N_G(N^2ML + N^3))$	691,200
DE	$O(N_{de}MNL)$	123,636
FNN	$O(N_fMNL)$	196,608
CNN	$O(MNLN_k(S_k + N_c/S_p))$	92,160
HNN	$O(MNLN_k(S_k + N_h^{[1]}/S_p) + N_h^{[2]}NP)$	36,864
SNN	$O(ML + N_s^{[1]} + N_s^{[2]})$	1,168

convolution kernels, size of convolutional kernel, and size of pooling, respectively. The typical numbers of multiplication operation are given under the condition of parameters that make the performance of the corresponding algorithm approximately optimal. The HNN-based algorithm has significantly reduced computational complexity compared with the existing Monte-Carlo method or deterministic equivalent method while achieving similar sum rate. It is worth mentioning that we can achieve the lowest complexity and the near-optimal sum rate simultaneously utilizing SNN in the case of $N = 2$.

C. Evaluation of Searching

Let $R_{th} = \theta \cdot R_{max}$, where parameter $\theta \in [0, 1]$ controls the degree of sum rate loss. Table III compares different fair scheduling algorithms, where $\theta = 0.8$, that is, the loss of sum rate is controlled at around 20%. The server ratio (SR) is defined as the percentage of the scheduled users. Compared with the sum rate maximization, the proportional fair criterion guarantees fairness at the expense of sum rate degradation while the Jain's fair method improves the Jain's index with less sum rate loss. In addition, the Jain's fair method achieves the highest server ratio, which implies fairness and stability. It is worth noting that the loss of sum rate for multi-cell scheduling can be controlled accurately by setting the parameter θ while the loss of sum rate is unpredictable and uncontrollable in proportional fair criterion.

Fig. 6 presents the tradeoff curve of Jain's fair method. The sum rate decreases as θ increases until it degenerates into

TABLE III
COMPARISON BETWEEN DIFFERENT SCHEDULING ALGORITHM

Algorithm	Sum Rate (b/s/Hz)	Jain's Index	SR (%)
Sum Rate Maximization	135.9493	0.0820	18.17
Proportional Fair	101.3178	0.1065	25.83
Jain's Fair	108.9174	0.2216	41.67

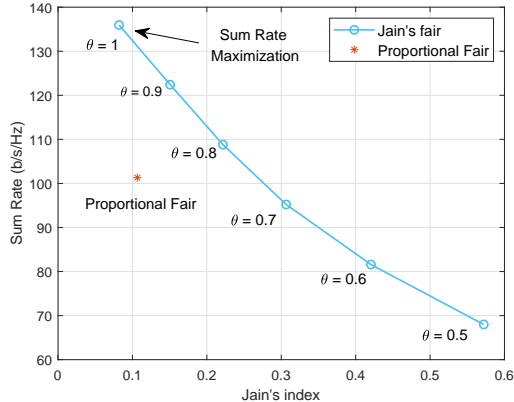


Fig. 6. The tradeoff curve of Jain's Fair method.

Jain's index maximization. The value of θ can be reasonably set according to practical demand to control the loss of the rate within a certain range to guarantee a minimum sum rate for communication and simultaneously to improve the fairness between users.

VI. CONCLUSION

In this paper, we have developed multi-cell scheduling with only statistical CSI in massive MIMO systems through a learning-to-compute strategy. In particular, a neural network is designed to learn directly the complex ergodic rate function, without resorting to the commonly used time-consuming Monte-Carlo or deterministic equivalent (DE) methods. Thanks to such a learning-to-compute strategy with substantially reduced online computational complexity, the simple K-Best algorithm can be employed for searching the best users to maximize the ergodic sum rate. Based on the simulation results, the computational complexity of the ergodic rate computation has been significantly reduced by employing the proposed neural network, compared with the existing Monte-Carlo or DE methods. To take the fairness among users into consideration, we have presented a multi-objective optimization problem, which simultaneously maximizes the ergodic sum rate and the Jains index, and further proposed the corresponding K-Best algorithm with low complexity. Compared with the traditional proportional fair criterion, the K-Best algorithm for Pareto optimal concerns with the fairness of a single schedule and is able to control the loss of sum rate accurately. For further avenues of research, it is worthy of making a profound study on learning the result of multi-cell scheduling directly through the existing statistical CSI without resorting to the scheduling algorithm.

APPENDIX A PROOF OF THEOREM 2

Denote by $h_{nm} = [\tilde{\mathbf{H}}_{k,j}]_{nm}$ and $k_m = [\mathbf{\Lambda}]_{mm}$, then the (n, m) -th elements of $\mathbf{X}_{k,j}$ is $[\mathbf{X}_{k,j}]_{nm} = \mathbb{E}(k_m|h_{nm}|^2)$, and the matrix $\tilde{\mathbf{H}}_{k,j} \mathbf{\Lambda} \tilde{\mathbf{H}}_{k,j}^H$ can be denoted by

$$\begin{aligned} \tilde{\mathbf{H}}_{k,j} \mathbf{\Lambda} \tilde{\mathbf{H}}_{k,j}^H &= \begin{bmatrix} \sum_m k_m |h_{1m}|^2 & \sum_i k_m h_{1m} h_{2m}^* \\ \sum_m k_m h_{2m} h_{1m}^* & \sum_i k_m |h_{2m}|^2 \end{bmatrix} \\ &= \begin{bmatrix} r & t^* \\ t & s \end{bmatrix}, \end{aligned} \quad (46)$$

and

$$\mathbb{E}(r) = \sum_m \mathbb{E}(k_m |h_{1m}|^2) = \sum_m [\mathbf{X}_{k,j}]_{1m}, \quad (47)$$

$$\mathbb{E}(s) = \sum_m \mathbb{E}(k_m |h_{2m}|^2) = \sum_m [\mathbf{X}_{k,j}]_{2m}, \quad (48)$$

$$\mathbb{E}(|t|^2) = \sum_m \mathbb{E}(k_m^2 |h_{1m}|^2 |h_{2m}|^2) = \sum_m \prod_n [\mathbf{X}_{k,j}]_{nm}. \quad (49)$$

According to the definition, λ_1, λ_2 are the roots of the following equation

$$\lambda^2 - (r + s)\lambda + rs - |t|^2 = 0. \quad (50)$$

As mentioned in section II, $\tilde{\mathbf{H}}$ is a random matrix with independent entries which are zero mean and arbitrary in amplitude, so it is easy to prove that

$$\mathbb{E}(\lambda_1 + \lambda_2) = \mathbb{E}(r + s) = \mathbb{E}(r) + \mathbb{E}(s), \quad (51)$$

$$\mathbb{E}(\lambda_1 \lambda_2) = \mathbb{E}(rs - |t|^2) = \mathbb{E}(r) \mathbb{E}(s) + \mathbb{E}(|t|^2). \quad (52)$$

By substituting the equations above, the proof is completed.

APPENDIX B PROOF OF LEMMA 1

- i) To derive the monotonicity of $f(x)$, we first compute its derivative

$$\frac{\partial \log \det(\mathbf{B} + x\mathbf{A})}{\partial x} = \text{tr} \left((\mathbf{B} + x\mathbf{A})^{-1} \mathbf{A} \right). \quad (53)$$

As \mathbf{A}, \mathbf{B} are positive definite matrices and $x \geq 0$, the matrix $\mathbf{B} + x\mathbf{A}$ is also a positive definite matrix. Thus, its inverse matrix satisfies $(\mathbf{B} + x\mathbf{A})^{-1} \succ \mathbf{0}$. Below we prove that the trace of product of two positive definite matrices is positive, i.e., $\text{tr}(\mathbf{AB}) > 0$. Owing to $\mathbf{B} \succ \mathbf{0}$, there exists an invertible matrix \mathbf{P} satisfying $\mathbf{B} = \mathbf{P}^H \mathbf{P}$. Thus, we can obtain that

$$\text{tr}(\mathbf{AB}) = \text{tr}(\mathbf{AP}^H \mathbf{P}) = \text{tr}(\mathbf{PAP}^H) > 0, \quad (54)$$

where the matrix \mathbf{PAP}^H is positive definite since it conjugates contract with \mathbf{A} . Thus, the same can be proved that the derivative $\text{tr}((\mathbf{B} + x\mathbf{A})^{-1} \mathbf{A}) > 0$, i.e., $f(x)$ increases monotonously with x on $x \geq 0$.

- ii) The derivative of $g(x)$ can be computed as

$$\frac{\partial g(x)}{\partial x} = \text{tr} \left(\left((\mathbf{B} + x\mathbf{A})^{-1} - (\mathbf{C} + x\mathbf{A})^{-1} \right) \mathbf{A} \right). \quad (55)$$

Owing to $\mathbf{B} + x\mathbf{A} \succ \mathbf{C} + x\mathbf{A}$, we have [47, 10.51 (a), [48]

$$(\mathbf{C} + x\mathbf{A})^{-1} - (\mathbf{B} + x\mathbf{A})^{-1} \succ \mathbf{0}. \quad (56)$$

As has been proved that the trace of product of two positive definite matrices is positive, we can obtain that $\frac{\partial g(x)}{\partial x} < 0$, i.e., $g(x)$ decreasing monotonously with x on $x \geq 0$.

APPENDIX C PROOF OF LEMMA 2

Denote by $\mathbf{\Lambda}_{k,\ell} = \rho_{k,\ell} \mathbf{\Delta}_{k,\ell}$, where $\rho_{i,\ell}$ is the power allocated to the k -th user by the ℓ -th BS, $\mathbf{\Delta}_{k,\ell}$ is normalized power allocation matrix satisfying $\text{tr}(\mathbf{\Delta}_{k,\ell}) = 1$. The achievable rate of k -th user in the j -th cell in (6) can be rewritten as

$$R_{k,j} = \mathbb{E} \left\{ \log \det \left(\mathbf{I} + \rho_{k,j} \tilde{\mathbf{H}}_{k,j,\ell} \mathbf{\Delta}_{k,j} \tilde{\mathbf{H}}_{k,j,\ell}^H + \sum_{(i,\ell) \neq (k,j)} \rho_{i,\ell} \tilde{\mathbf{H}}_{k,j,\ell} \mathbf{\Delta}_{i,\ell} \tilde{\mathbf{H}}_{k,j,\ell}^H \right) \right\} - \mathbb{E} \left\{ \log \det \left(\mathbf{I} + \sum_{(i,\ell) \neq (k,j)} \rho_{i,\ell} \tilde{\mathbf{H}}_{k,j,\ell} \mathbf{\Delta}_{i,\ell} \tilde{\mathbf{H}}_{k,j,\ell}^H \right) \right\}, \quad (57)$$

and the maximization problem in (35) can be rewritten as

$$\begin{aligned} & \max_{\rho_{1,1}, \dots, \rho_{K,L}, \mathbf{\Delta}_{1,1}, \dots, \mathbf{\Delta}_{K,L}} \min_{k,j} (\omega_{k,j} R_{k,j}), \\ & \text{s.t.} \quad \sum_{k=1}^K \rho_{k,\ell} \leq P_\ell, \\ & \quad \text{tr}(\mathbf{\Delta}_{k,\ell}) = 1, \\ & \quad \rho_{k,\ell} \mathbf{\Delta}_{k,\ell} \succeq \mathbf{0}. \end{aligned} \quad (58)$$

As the weights have no effect on the proof procedure, we might as well set $\omega_{k,j} = 1$ for conciseness. Below we give the proof with reduction to absurdity.

Denote by $(\rho_{1,1}^\diamond, \dots, \rho_{K,L}^\diamond, \mathbf{\Delta}_{1,1}^\diamond, \dots, \mathbf{\Delta}_{K,L}^\diamond)$ the optimal solution of problem (58), $(R_{1,1}^\diamond, \dots, R_{K,L}^\diamond)$ as the corresponding optimal rates. Assuming that the optimal rates are not completely equal, we might as well set $R_{m,n}^\diamond$ as maximum rate and $R_{a,b}^\diamond$ as minimum rate, i.e.,

$$\min_{k,j} (R_{k,j}^\diamond) = R_{a,b}^\diamond < R_{m,n}^\diamond = \max_{k,j} (R_{k,j}^\diamond). \quad (59)$$

Invoking Lemma 1, the rate $R_{k,j}$ monotonically increases with the power allocated to itself $\rho_{k,j}$, and the rate $R_{k,j}$ monotonically decreases with the power allocated to other user $\rho_{i,\ell}$. Based on these properties, there always exists a sufficiently small ε to establish a solution $(\rho_{1,1}^\diamond, \dots, \rho_{m,n}^\diamond - \varepsilon, \dots, \rho_{K,L}^\diamond, \mathbf{\Delta}_{1,1}^\diamond, \dots, \mathbf{\Delta}_{K,L}^\diamond)$ whose corresponding rates $(\hat{R}_{1,1}, \dots, \hat{R}_{K,L})$ satisfy

$$\hat{R}_{k,j} = \begin{cases} R_{k,j}^\diamond - \varepsilon_{k,j}, & (k,j) = (m,n) \\ R_{k,j}^\diamond + \varepsilon_{k,j}, & (k,j) \neq (m,n) \end{cases}, \quad (60)$$

where variables $\varepsilon_{k,j} > 0$. As the rate is continuous with respect to $\rho_{k,j}$, the variables $\varepsilon_{k,j}$ are sufficiently small to satisfy

$$\hat{R}_{a,b} = R_{a,b}^\diamond + \varepsilon_{a,b} < R_{m,n}^\diamond - \varepsilon_{m,n} = \hat{R}_{m,n}. \quad (61)$$

This means the user with the minimum rate differs from (m,n) -th user. As the rates of other users increase, the minimum rate increases, i.e.,

$$\min_{k,j} (\hat{R}_{k,j}) \geq \min_{k,j} (R_{k,j}^\diamond), \quad (62)$$

which is contrary to that $(R_{1,1}^\diamond, \dots, R_{K,L}^\diamond)$ are the optimal rates. Thus, the optimal rates are completely equal. This completes the proof.

REFERENCES

- [1] J. Shi, W. Wang, J. Wang, and X.-Q. Gao, "Machine learning assisted user-scheduling method for massive MIMO system," in *Conf. Wireless Commun. Signal Process. (WCSP)*, Oct. 2018, pp. 1–6.
- [2] E. G. Larsson, O. Edfors, F. Tufvesson, and T. L. Marzetta, "Massive MIMO for next generation wireless systems," *IEEE Commun. Mag.*, vol. 52, no. 2, pp. 186–195, Feb. 2014.
- [3] L. Lu, G. Y. Li, A. L. Swindlehurst, A. Ashikhmin, and R. Zhang, "An overview of massive mimo: Benefits and challenges," *J. Sel. Signal Process.*, vol. 8, no. 5, Oct 2014.
- [4] T. L. Marzetta, "Noncooperative cellular wireless with unlimited numbers of base station antennas," *IEEE Trans. Wireless Commun.*, vol. 9, no. 11, pp. 3590–3600, Nov. 2010.
- [5] D. Ciuonzo, P. S. Rossi, and S. Dey, "Massive MIMO channel-aware decision fusion," *IEEE Trans. Signal Process.*, vol. 63, no. 3, pp. 604–619, 2015.
- [6] A. Shirazinia, S. Dey, D. Ciuonzo, and P. S. Rossi, "Massive MIMO for decentralized estimation of a correlated source," *IEEE Trans. Signal Process.*, vol. 64, no. 10, pp. 2499–2512, 2016.
- [7] L. Liu and W. Yu, "Massive connectivity with massive MIMO - part I: device activity detection and channel estimation," *IEEE Trans. Signal Process.*, vol. 66, no. 11, pp. 2933–2946, 2018.
- [8] H. Q. Ngo, M. Matthaiou, T. Q. Duong, and E. G. Larsson, "Uplink performance analysis of multicell MU-MIMO systems with ZF receivers," *IEEE Trans. Veh. Technol.*, vol. 62, no. 9, pp. 4471–4483, Nov. 2013.
- [9] J. Hoydis, S. ten Brink, and M. Debbah, "Massive MIMO in the UL/DL of cellular networks: How many antennas do we need?" *IEEE J. Sel. Areas Commun.*, vol. 31, no. 2, pp. 160–171, Feb. 2013.
- [10] N. Jindal, "MIMO broadcast channels with finite-rate feedback," *IEEE Trans. Inf. Theory*, vol. 52, no. 11, pp. 5045–5060, Nov. 2006.
- [11] X. Song, S. Haghghatshoar, and G. Caire, "A scalable and statistically robust beam alignment technique for millimeter-wave systems," *IEEE Trans. Wireless Commun.*, vol. 17, no. 7, pp. 4792–4805, July 2018.
- [12] C. Sun, X.-Q. Gao, S. Jin, M. Matthaiou, Z. Ding, and C. Xiao, "Beam division multiple access transmission for massive MIMO communications," *IEEE Trans. Commun.*, vol. 63, no. 6, pp. 2170–2184, Jun. 2015.
- [13] M. N. Boroujerdi, S. Haghghatshoar, and G. Caire, "Low-complexity statistically robust precoder/detector computation for massive mimo systems," *IEEE Trans. Wireless Commun.*, vol. 17, no. 10, pp. 6516–6530, Oct 2018.
- [14] L. You, X.-Q. Gao, A. L. Swindlehurst, and W. Zhong, "Channel acquisition for massive MIMO-OFDM with adjustable phase shift pilots," *IEEE Trans. Signal Process.*, vol. 64, no. 6, pp. 1461–1476, Mar. 2016.
- [15] A.-A. Lu, X.-Q. Gao, and C. Xiao, "Free deterministic equivalents for the analysis of MIMO multiple access channel," *IEEE Trans. Inf. Theory*, vol. 62, no. 8, pp. 4604–4629, Aug. 2016.
- [16] Y. Liu, H. Chen, and L. Wang, "Secrecy capacity analysis of artificial noisy MIMO channels - an approach based on ordered eigenvalues of wishart matrices," *IEEE Trans. Inf. Forensics Security*, vol. 12, no. 3, pp. 617–630, Mar. 2017.
- [17] W. Weichselberger, M. Herdin, H. Ozcelik, and E. Bonek, "A stochastic mimo channel model with joint correlation of both link ends," *IEEE Trans. Wireless Commun.*, vol. 5, no. 1, pp. 90–100, Jan 2006.
- [18] C. Sun, X.-Q. Gao, and Z. Ding, "BDMA in multicell massive MIMO communications: Power allocation algorithms," *IEEE Trans. Signal Process.*, vol. 65, no. 11, pp. 2962–2974, Jun. 2017.
- [19] D. Chizhik, G. J. Foschini, M. J. Gans, and R. A. Valenzuela, "Key-holes, correlations, and capacities of multielement transmit and receive antennas," *IEEE Trans. Wireless Commun.*, vol. 1, no. 2, pp. 361–368, Aug. 2002.
- [20] J. Shin and J. Moon, "Weighted sum rate maximizing transceiver design in mimo interference channel," in *IEEE Global Telecommun. Conf (GLOBECOM)*, Dec 2011, pp. 1–5.

- [21] S. S. Christensen, R. Agarwal, E. de Carvalho, and J. M. Cioffi, "Weighted sum-rate maximization using weighted MMSE for MIMO-BC beamforming design," *IEEE Trans. Wireless Commun.*, vol. 7, no. 12-1, pp. 4792–4799, Dec. 2008.
- [22] W. Cui, K. Shen, and W. Yu, "Spatial deep learning for wireless scheduling," *IEEE J. Sel. Areas Commun.*, vol. 37, no. 6, pp. 1248–1261, 2019.
- [23] C. H. Papadimitriou and K. Steiglitz, *Combinatorial optimization: algorithms and complexity*. Courier Corporation, 1998.
- [24] I. J. Goodfellow, Y. Bengio, and A. Courville, *Deep Learning*. Cambridge, MA, USA: MIT Press, 2016.
- [25] K. Hornik, "Approximation capabilities of multilayer feedforward networks," *Neural Networks*, vol. 4, no. 2, pp. 251–257, 1991.
- [26] G. Cybenko, "Approximation by superpositions of a sigmoidal function," *Math. Control, Signals and Systems*, vol. 2, no. 4, pp. 303–314, 1989.
- [27] D.-X. Zhou, "Universality of deep convolutional neural networks," *Applied and Comp. Harmonic Analysis*, 2019.
- [28] B. O. Koopman, "On distributions admitting a sufficient statistic," *Trans. American Math. Society*, vol. 39, no. 3, pp. 399–409, 1936.
- [29] C. Zhang, P. Patras, and H. Haddadi, "Deep learning in mobile and wireless networking: A survey," *IEEE Commun. Surveys and Tut.*, vol. 21, no. 3, pp. 2224–2287, 2019.
- [30] A. Krizhevsky, I. Sutskever, and G. E. Hinton, "Imagenet classification with deep convolutional neural networks," in *Advances in Neural Info. Proc. Systems*, 2012, pp. 1097–1105.
- [31] D. C. Ciresan, U. Meier, and J. Schmidhuber, "Multi-column deep neural networks for image classification," in *IEEE Conf. Comp. Vision and Pattern Recog. (CVPR)*, Jul. 2012, pp. 3642–3649.
- [32] N. Srivastava, G. Hinton, A. Krizhevsky, I. Sutskever, and R. Salakhutdinov, "Dropout: a simple way to prevent neural networks from overfitting," *J. Machine Learning Research*, vol. 15, no. 1, pp. 1929–1958, 2014.
- [33] L. Liu, Young-Han Nam, and J. Zhang, "Proportional fair scheduling for multi-cell multi-user mimo systems," in *Annual Conf. Info. Sci. and Systems (CISS)*, March 2010, pp. 1–6.
- [34] E. Liu and K. K. Leung, "Proportional fair scheduling: Analytical insight under rayleigh fading environment," in *IEEE Wireless Commun. & Network. Conf. (WCNC)*, Apr. 2008, pp. 1883–1888.
- [35] H. T. Cheng and W. Zhuang, "An optimization framework for balancing throughput and fairness in wireless networks with qos support," *IEEE Trans. Wireless Commun.*, vol. 7, no. 2, pp. 584–593, Feb. 2008.
- [36] C. Joe-Wong, S. Sen, T. Lan, and M. Chiang, "Multi-resource allocation: Fairness-efficiency tradeoffs in a unifying framework," in *IEEE Conf. Comp. Commun. (INFOCOM)*, May. 2012, pp. 1206–1214.
- [37] T. Lan, D. Kao, M. Chiang, and A. Sabharwal, "An axiomatic theory of fairness in network resource allocation," in *IEEE Conf. Comp. Commun. (INFOCOM)*, March 2010, pp. 1–9.
- [38] F. Malucelli, "A polynomially solvable class of quadratic semi-assignment problems," *Europ. J. Operat. Res.*, vol. 91, no. 3, pp. 619–622, 1996.
- [39] P. Kleinschmidt and H. Schannath, "A strongly polynomial algorithm for the transportation problem," *Math. Program.*, vol. 68, no. 1-3, pp. 1–13, 1995.
- [40] M. Stojnic, H. Vikalo, and B. Hassibi, "Rate maximization in multi-antenna broadcast channels with linear preprocess," *IEEE Trans. Wireless Commun.*, vol. 5, no. 9, pp. 2338–2342, Sept. 2006.
- [41] A. B. Sediq, R. H. Gohary, R. Schoenen, and H. Yanikomeroglu, "Optimal tradeoff between sum-rate efficiency and jain's fairness index in resource allocation," *IEEE Trans. Wireless Commun.*, vol. 12, no. 7, pp. 3496–3509, Jun. 2013.
- [42] S. Boyd and L. Vandenberghe, *Convex Optimization*. New York, NY, USA: Cambridge University Press, 2004.
- [43] J. Rubio, A. Pascual-Iserte, D. P. Palomar, and A. Goldsmith, "Joint optimization of power and data transfer in multiuser MIMO systems," *IEEE Trans. Signal Process.*, vol. 65, no. 1, pp. 212–227, Jan. 2017.
- [44] Y. J. Bultitude, and T. Rautiainen, "IST-4-027756 WINNER II D1.1.2 V1.2 WINNER II Channel Models," Sept. 2007.
- [45] X. Sun, C. Wu, X. Gao, and G. Y. Li, "Fingerprint-based localization for massive MIMO-OFDM system with deep convolutional neural networks," *IEEE Trans. Veh. Technol.*, vol. 68, no. 11, pp. 10846–10857, 2019.
- [46] C. Tan, F. Sun, T. Kong, W. Zhang, C. Yang, and C. Liu, "A survey on deep transfer learning," in *Int. Conf. Artificial Neural Networks (ICANN)*, vol. 11141. Springer, 2018, pp. 270–279.
- [47] G. A. F. Seber, *A Matrix Handbook for Statisticians*. Hoboken, NJ, USA: John Wiley Sons, Inc., 2007.
- [48] P. J. Dhrymes, *Mathematics for Econometrics*. New York, NY, USA: Springer-Verlag, 2000.



Junchao Shi (S'18) received the B.E. degree in communication engineering from Xidian University, Xi'an, China, in 2016. He is currently working towards the Ph.D degree in the National Mobile Communications Research Laboratory, Southeast University, Nanjing, China. His research interests are mainly on communications, signal processing, and information theory, machine learning with emphasis on massive MIMO communications.



Wenjin Wang (M'14) received the Ph.D. degree in communication and information systems from Southeast University, Nanjing, China, in 2011. From 2010 to 2014, he was with the School of System Engineering, University of Reading, Reading, U.K. He is currently an Associate Professor with the National Mobile Communications Research Laboratory, Southeast University. His research interests include advanced signal processing for future wireless communications and satellite communications. He was awarded a Best Paper Award at IEEE WCSP09.

He was also awarded the first grade Technological Invention Award of the State Education Ministry of China in 2009.



Xinpeng Yi (S'12-M'15) received his Ph.D. degree in Electronics and Communications in 2015 from Télécom ParisTech, Paris, France. He is currently a Lecturer (Assistant Professor) at the Department of Electrical Engineering and Electronics of the University of Liverpool, United Kingdom. Prior to Liverpool, he was a research associate at Technische Universität Berlin, Berlin, Germany from 2014 to 2017, a research assistant at EURECOM, Sophia Antipolis, France from 2011 to 2014, and a research engineer at Huawei Technologies, Shenzhen, China from 2009 to 2011. His main research interests include information theory, graph theory, and machine learning, as well as their applications in wireless communications and artificial intelligence.



Jiaheng Wang (M'10–SM'14) received the Ph.D. degree in electronic and computer engineering from the Hong Kong University of Science and Technology, Kowloon, Hong Kong, in 2010, and the B.E. and M.S. degrees from the Southeast University, Nanjing, China, in 2001 and 2006, respectively.

He is currently a Full Professor at the National Mobile Communications Research Laboratory (N-CRL), Southeast University, Nanjing, China. From 2010 to 2011, he was with the Signal Processing Laboratory, KTH Royal Institute of Technology, Stockholm, Sweden. He also held visiting positions at the Friedrich Alexander University Erlangen-Nrnberg, Nrnberg, Germany, and the University of Macau, Macau. His research interests include optimization in signal processing and wireless communications.

Dr. Wang has published more than 100 articles on international journals and conferences. From 2014 to 2018, he served as an Associate Editor for the IEEE Signal Processing Letters. From 2018, he serves as a Senior Area Editor for the IEEE Signal Processing Letters. He was a recipient of the Humboldt Fellowship for Experienced Researchers and the best paper awards of IEEE GLOBECOM 2019, ADHOCNETS 2019, and WCSP 2014.

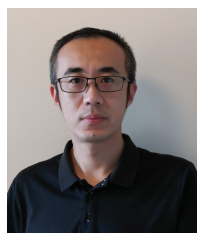


Xiqi Gao (S'92–AM'96–M'02–SM'07–F'15) received the Ph.D. degree in electrical engineering from Southeast University, Nanjing, China, in 1997.

He joined the Department of Radio Engineering, Southeast University, in April 1992. Since May 2001, he has been a professor of information systems and communications. From September 1999 to August 2000, he was a visiting scholar at Massachusetts Institute of Technology, Cambridge, and Boston University, Boston, MA. From August 2007 to July 2008, he visited the Darmstadt University

of Technology, Darmstadt, Germany, as a Humboldt scholar. His current research interests include broadband multi-carrier communications, MIMO wireless communications, channel estimation and turbo equalization, and multi-rate signal processing for wireless communications. From 2007 to 2012, he served as an Editor for the IEEE TRANSACTIONS ON WIRELESS COMMUNICATIONS. From 2009 to 2013, he served as an Associate Editor for the IEEE TRANSACTIONS ON SIGNAL PROCESSING. From 2015 to 2017, he served as an Editor for the IEEE TRANSACTIONS ON COMMUNICATIONS.

Dr. Gao received the Science and Technology Awards of the State Education Ministry of China in 1998, 2006 and 2009, the National Technological Invention Award of China in 2011, and the 2011 IEEE Communications Society Stephen O. Rice Prize Paper Award in the field of communications theory.



Qing Liu received the B.S. and M.S. degrees, from the department of Information Science & Electronic Engineering, Zhejiang University, in 2004 and 2006, respectively. Since 2006, he joined Huawei Technology Co., Ltd and worked as a senior engineer. His research interests include both L1 and L2 algorithm design, like advanced receiver, architecture of base-band algorithm, AI in wireless system and so on.



Geoffrey Ye Li (S'93–M'95–SM'97–F'06) is a Professor at Georgia Institute of Technology, Atlanta, GA. Before moving to Georgia Tech, he was with AT&T Labs - Research at Red Bank, New Jersey, as a Senior and then a Principal Technical Staff Member, from 1996 to 2000, and a Post-Doctoral Research Associate with the University of Maryland at College Park, Maryland, from 1994 to 1996. His general research interests include statistical signal processing and machine learning for wireless communications. In these areas, he has published over

500 journal and conference papers in addition to over 40 granted patents. His publications have been cited over 42,000 times and he has been recognized as the Worlds Most Influential Scientific Mind, also known as a Highly Cited Researcher, by Thomson Reuters almost every year.

Dr. Geoffrey Ye Li was awarded IEEE Fellow for his contributions to signal processing for wireless communications in 2005. He won several prestigious awards from IEEE Signal Processing Society (Donald G. Fink Overview Paper Award in 2017), IEEE Vehicular Technology Society (James Evans Avant Garde Award in 2013 and Jack Neubauer Memorial Award in 2014), and IEEE Communications Society (Stephen O. Rice Prize Paper Award in 2013, Award for Advances in Communication in 2017, and Edwin Howard Armstrong Achievement Award in 2019). He also received 2015 Distinguished Faculty Achievement Award from the School of Electrical and Computer Engineering, Georgia Tech.

He has been involved in editorial activities for over 20 technical journals, including the founding Editor-in-Chief of IEEE 5G Tech Focus and the founding Editor-in-Chief of IEEE JSAC Special Series on ML in Communications and Networking. He has organized and chaired many international conferences, including technical program vice-chair of the IEEE ICC03, technical program co-chair of the IEEE SPAWC11, general co-chair of the IEEE GlobalSIP14, technical program co-chair of the IEEE VTC16 (Spring), general co-chair of the IEEE VTC19 (Fall), and the IEEE SPAWC20.